Design of Flanged RF Shield for Mitigation of RF and Gradient Coil Interactions

Muhammad Hassan Chishti[1], Jean-Baptiste Mathieu[1], Joseph E Piel[1], Desmond T.B. Yeo[1], Christopher J Hardy[1], Dominic Graziani[1], and Seung-Kyun Lee[1]
[1]*GE Global Research Center, Niskayuna, New York, United States*

Target Audience: Researchers interested in improved radiofrequency (RF) shield design and asymmetric gradient coils.

Introduction: RF shields are an integral part of MRI scanners as they isolate and decouple the gradient coils and main-magnet resistive shims from the RF transmit coil. RF fields generated by the transmit coil can exhibit spurious resonances arising from interactions with the gradient windings [1-2], resulting in added RF losses [3]. These losses degrade the quality factor (Q) of the RF coil, resulting in increased RF power requirements. RF fields are normally shielded in the radial direction beyond the boundaries of the RF shield, thus eliminating undesired interactions with the gradient coils and other conductive structures. Recently, we reported the construction of an asymmetric head-only gradient coil for a dedicated neuroimaging scanner at 3 T [4]. Due to the asymmetric design, a conventional RF shield lining the inner surface of the gradient coil provides insufficient RF isolation between the transmit coil and the gradient coils. In this work, we analyze the leakage field from an improved, flanged RF shield that reduces the coupling with the gradient windings. Results from full-wave electromagnetic (EM) simulations are presented along with bench-top measurements.

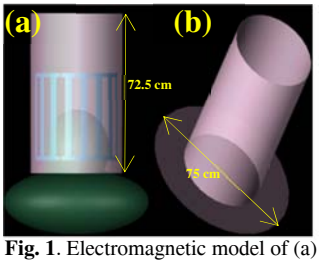

Fig. 1. Electromagnetic model of (a) RF shield with RF coil and phantom, and (b) flanged RF shield

Methods: ***FDTD modeling*** A head-size 16-rung 3T high-pass birdcage head coil (inner dia = 37.5 cm, L = 40 cm) was modeled and tuned loaded (head-size sphere phantom on a shoulder-simulating ellipsoid) to 128 MHz using xFDTD (Remcom, State College, PA). The coil was driven in quadrature mode with four ports having equal voltage magnitude and phase values of 0°, 90°, 180°, and 270°. The FDTD cell size for the coil, shield, and background was set to 3mm × 3mm × 3mm. The coil was tuned under the following two conditions: (A) with a conventional, non-flanged shield, and (B) with a flanged shield. Each of the above two cases were further divided into two subsets: (i) no gradient coils present, and (ii) all gradients (X,Y,Z - both primary and secondary) present. The gradient coils here were passive copper windings without driving circuits. The gradients were included for two reasons: (i) to define the spatial positions to measure the extent of the field leakage, and (ii) to identify any induced currents on the gradient conductors. The height of both conventional and flanged RF shields (Fig. 1a) was 72.5 cm and diameter 42 cm. The flanged shield (Fig. 1b) had an outer diameter of 75 cm. Both shields were also built and tested on the bench (Fig. 4).

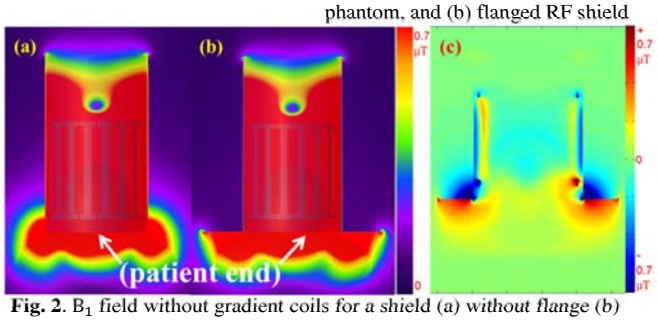

Fig. 2. B_1 field without gradient coils for a shield (a) without flange (b) with flange. (c) difference map = (B_1 with flange - B_1 without flange)

Results and Discussion: Fig. 2 shows the coronal view of B_1 field at isocenter without (Fig. 2a) and with the flange (Fig. 2b) present. B_1 field mitigation due to the flanged shield can be assessed by the difference image (Figs. 2c and 3c) obtained from the post-processing of B_1 using the equation: $difference = (B_1\ with\ flange - B_1\ without\ flange)$. Negative values of the difference map, as indicated by the color scale (Fig. 2c and 3c), suggest mitigation of the leakage field in proximity of gradient coils due to the flange. In the absence of the circular end flange, B_1 fields leak beyond the edges of the shield towards the patient side. This leakage field can impinge on the gradients, inducing undesired eddy currents and resonances, which lowers the performance of the RF coil. Fig. 3 shows the same types of fields as in Fig. 2, except with the gradient windings present. The B_1 field leakage beyond the shield edge and over to the gradients was lowered considerably as evident from the difference map (Fig. 3c). Note that both scenarios presented in Figs. 2 and 3 were normalized to the same amount of input power (100 watts). The B_1 efficiency of the RF coil (Table 1) drops by only 0.9% when the flange is introduced. The flanged RF shield was constructed and the Q of the RF coil was measured on the bench (Fig. 4) with and without the flanged shield. The Q of the unloaded coil with the flanged RF shield (Fig. 4a) was 185 (Fig. 4b), showing large improvement over the same RF coil with the conventional shield (Fig. 4c), whose Q was measured at 50 (Figs. 4d).

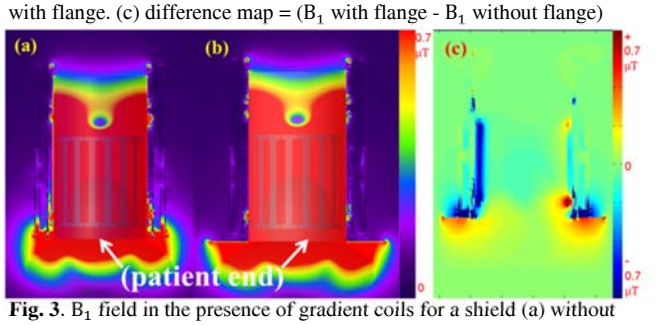

Fig. 3. B_1 field in the presence of gradient coils for a shield (a) without flange (b) with flange. (c) difference map = (B_1 with flange - B_1 without flange)

	Without Flanged Shield	Flanged RF Shield
With Gradients	7.0021 μT	6.9326 μT
No Gradients	7.0631 μT	6.9310 μT

Table 1. B_1 field efficiency at the isocenter normalized to the same input power

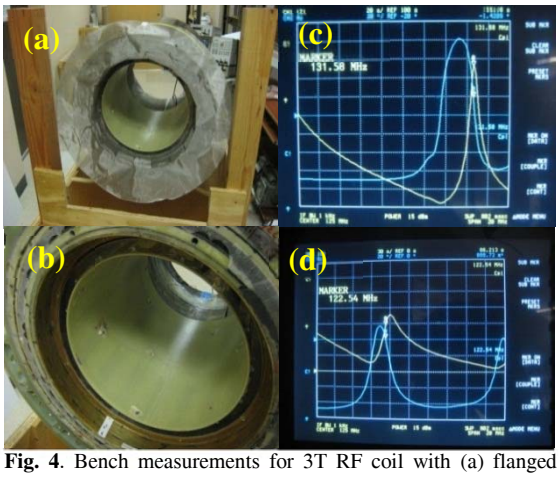

Fig. 4. Bench measurements for 3T RF coil with (a) flanged shield and (b) conventional shield. Quality factor was c) 185 for RF coil with flanged shield and (d) 50 for RF coil with conventional shield.

Conclusions: EM modeling results and bench measurements were presented for an RF shield with a circular end-flange attached towards the patient end to prevent the B_1 field leakage to the gradient coils. Results showed that the proposed design was effective in curbing the leakage field, especially towards part of the gradient windings that were in close proximity to the patient end of the RF coil.

Acknowledgment: This work was supported in part by the NIH grant 5R01EB010065.

References: [1] Hayes CE, Eash MG. U.S. patent 4,642,569; 1987. [2] Alecci M, et al. Magnetic Resonance in Medicine 48:404-407; 2002. [3] Roemer PB, et al. U.S. patent 4,879,515; 1989. [4] Mathieu et al., ISMRM 21 (2013), 2708.